Bioactive Materials 6 (2021) 2667–2675

Contents lists available at ScienceDirect

Bioactive Materials

journal homepage: www.sciencedirect.com/journal/bioactive-materials

# Ionic liquid-loaded microcapsules doped into dental resin infiltrants

Marla Cuppini [a], Isadora Martini Garcia [a], Virgínia Serra de Souza [b], Kelly Cristine Zatta [c], Fernanda Visioli [d], Vicente Castelo Branco Leitune [a], Sílvia Stanisçuazki Guterres [e], Jackson Damiani Scholten [b,**], Fabrício Mezzomo Collares [a,*]

[a] Department of Dental Materials, School of Dentistry, Federal University of Rio Grande do Sul, Ramiro Barcelos Street, 2492, Rio Branco, 90035-003, Porto Alegre, RS, Brazil
[b] Laboratory of Molecular Catalysis, Institute of Chemistry, Federal University of Rio Grande do Sul, Bento Gonçalves Avenue, 9500, Agronomia, 91501-970, Porto Alegre, RS, Brazil
[c] Cosmetology and Pharmaceutical Nanotechnology Laboratory, School of Pharmaceutical Sciences, Universidade Federal do Rio Grande do Sul, Av. Ipiranga 2752, 90610-000, Porto Alegre, RS, Brazil
[d] Oral Pathology Department, School of Dentistry, Federal University of Rio Grande do Sul, Rua Ramiro Barcelos, 2492, Rio Branco, 90035-003, Porto Alegre, RS, Brazil
[e] Cosmetology Laboratory, School of Pharmaceutical Sciences, Universidade Federal do Rio Grande do Sul, Av. Ipiranga 2752, 90610-000, Porto Alegre, RS, Brazil

ARTICLE INFO

*Keywords:*
Surface properties
Dental caries
Stress
Mechanical
Drug delivery systems
Polymers

ABSTRACT

Resin infiltrants have been effectively applied in dentistry to manage non-cavitated carious lesions in proximal dental surfaces. However, the common formulations are composed of inert methacrylate monomers. In this study, we developed a novel resin infiltrant with microcapsules loaded with an ionic liquid (MC-IL), and analyzed the physical properties and cytotoxicity of the dental resin. First, the ionic liquid 1-*n*-butyl-3-methylimidazolium bis(trifluoromethanesulfonyl)imide (BMI.$NTf_2$) was synthesized. BMI.$NTf_2$ has previously shown antibacterial activity in a dental resin. Then, MC-IL were synthesized by the deposition of a preformed polymer. The MC-IL were analyzed for particle size and de-agglomeration effect via laser diffraction analysis and shape via scanning electron microscopy (SEM). The infiltrants were formulated, and the MC-IL were incorporated at 2.5%, 5%, and 10 wt%. A group without MC-IL was used as a control. The infiltrants were evaluated for ultimate tensile strength (UTS), contact angle, surface free energy (SFE), and cytotoxicity. The MC-IL showed a mean particle size of 1.64 (±0.08) μm, shriveled aspect, and a de-agglomeration profile suggestive of nanoparticles' presence in the synthesized powder. There were no differences in UTS among groups ($p > 0.05$). The incorporation of 10 wt% of MC-IL increased the contact angle ($p < 0.05$), while the addition from 5 wt% reduced the SFE in comparison to the control group ($p < 0.05$). The human cell viability was above 90% for all groups ($p > 0.05$). The incorporation of microcapsules as a drug-delivery system for ionic liquids may be a promising strategy to improve dental restorative materials.

## 1. Introduction

Dental caries is a high prevalent disease worldwide [1], leading to pain, loss of dental tissues or teeth, and negatively impacting the quality of life [2]. The prevalence of dental caries in proximal surfaces encompass more than 50% of caries lesions [3]. Early intervention in this disease reduces the chances of increasing the loss of dental tissues. The primary strategy to treat incipient enamel caries lesion involves the nonoperative management by topical fluoride application, patients' education for oral hygiene improvement, and appropriate diet [4,5]. When the lesion extension and the chances of surface breakdown increase, the development of biocompatible materials to hinder the lesions is recommended [6].

The use of resin infiltrants is an approach to treat superficial

Peer review under responsibility of KeAi Communications Co., Ltd.
* Corresponding author.
** Corresponding author.
*E-mail addresses:* marla.cupini@ufrgs.br (M. Cuppini), isadora.garcia@ufrgs.br (I.M. Garcia), vivi_qui@hotmail.com (V.S. de Souza), kellycriz@hotmail.com (K.C. Zatta), fevisioli@gmail.com (F. Visioli), vicente.leitune@ufrgs.br (V.C.B. Leitune), silvia.guterres@ufrgs.br (S.S. Guterres), jackson.scholten@ufrgs.br (J.D. Scholten), fabricio.collares@ufrgs.br (F.M. Collares).

https://doi.org/10.1016/j.bioactmat.2021.02.002
Received 22 October 2020; Received in revised form 2 January 2021; Accepted 1 February 2021
Available online 12 February 2021

proximal carious lesions [7,8]. Infiltrants are light-curable resins that occlude the porous of lesions, sealing inside the lesion body and its surface [9]. In comparison to sealants, resin infiltrants have a higher flow because it lacks inorganic filler. As an interesting advantage of infiltrants, there is no need for an extra clinical step of tooth separation to be placed on proximal dental areas, decreasing procedure time and improving patient comfort [10]. A previous randomized clinical trial [11] showed that proximal lesions infiltration combined with diet and hygiene instructions arrested clinically and radiographically more lesions (5% of lesions progression) in comparison to diet and hygiene instructions alone after eighteen months (31% of lesions progression). It indicated that resin infiltrants' use led to a relative risk reduction of 83% (95% CI 67–91%) [11].

Even though resin infiltrants indicate clinically significant results by hampering carious progression, a range of patients did not show improvement (9–33%) [11]. Common methacrylates used to formulate restorative materials, such as triethylene glycol dimethacrylate (TEGDMA) and bisphenol A-glycidyl methacrylate (Bis-GMA), do not present antimicrobial activity [12]. The antimicrobial property could improve enamel caries prevention by reducing biofilm formation [13], which may positively impact patients with a high risk of caries that are not being benefited from enamel infiltration [14]. Antimicrobial agents have been added to resin infiltrants to improve their biological properties and increase their protective effect. Previous studies incorporated silver nanoparticles (AgNP) [15], quaternary ammonium methacrylate [16], cationic molecules [17], and chlorhexidine into resin infiltrants formulation. AgNP were incorporated into a commercial infiltrant at 5.5 wt% and tested regarding enamel's penetrability [15]. In this *ex vivo* study, AgNP did not alter the infiltration on proximal enamel caries [15]. Cationic molecules such as dimethylaminododecyl methacrylate (DMADDM) [16], guanidine hydrochloride [17], and chlorhexidine [18] were tested regarding antibacterial activity and showed promising results.

As a novel antimicrobial agent for dental resins, ionic liquids (ILs) have been proposed [19–21]. ILs, mainly those based on the imidazolium cation, are organic salts with low melting point and 3D structural organization due to the imidazolium cation interaction with a weakly coordinating anion [22,23]. The antibacterial role of IL cation is via the interaction with the negatively charged species of bacterial membrane and wall, acting via direct contact with the microorganism [22]. In particular, the anion bis(trifluoromethanesulfonyl)imide ($NTf_2$) offers hydrophobicity to the IL, which may increase its antibacterial property [22]. The use of ILs has been highlighted because of their possible advantages over common salts. Salts are about 50% of active drugs used for pharmacological processes [24]. However, these materials suffer crystal polymorphism in pharmaceutical compounds [24]. ILs, on the other hand, are considered molten salts since they are found liquid in temperatures below 100 °C. Therefore, polymorphism's common problem can be overcome using active drugs composed of ILs [24]. Furthermore, ILs are the ultimate solution to defeat antimicrobial resistance due to the possibility of tuning them by changing their counterions [22]. These properties make them possible advantageous compared to metallic oxides and classical antimicrobial agents, such as chlorhexidine.

Recently, an ionic liquid with imidazolium cation and $NTf_2$ anion, 1-*n*-butyl-3-methylimidazolium bis(trifluoromethanesulfonyl)imide (BMI.$NTf_2$) was used as an antibacterial agent for an experimental orthodontic adhesive against *Streptococcus mutans* [21]. In the previous research [21], BMI.$NTf_2$ was free in the adhesive. The design of dental resins with drug delivery systems carrying ILs could be an advantage to maintain reliable physicochemical and antibacterial properties over time [25,26]. However, there are no reports about the encapsulation of ILs in dental materials. The aim of this study was to synthesize microcapsules loaded with the ionic liquid (MC-IL) 1-*n*-butyl-3-methylimidazolium bis(trifluoromethanesulfonyl)imide (BMI.$NTf_2$) and evaluate the addition of MC-IL in the physical, chemical, and cytotoxicity properties of experimental resin infiltrants.

## 2. Materials and methods

### 2.1. Synthesis of ionic liquid-loaded microcapsules (MC-IL)

To synthesize ionic liquid-loaded microcapsules (MC-IL), the ionic liquid 1-*n*-butyl-3-methylimidazoilium bis(trifluoromethanesulfonyl) imide (BMI.$NTf_2$) was synthesized according to previous study [21,27] (Fig. 1). All reagents for the ionic liquid synthesis were purchased from Sigma-Aldrich Chemical (St. Louis, MO, USA). Three steps were performed to obtain butyl methanesulfonate (1st step), 1-*n*-butyl-3-methylimidazolium methanesulfonate (2nd step), and finally, the ionic liquid 1-*n*-butyl-3-methylimidazolium bis(trifluoromethanesulfonyl) imide (BMI.$NTf_2$) used to synthesize the microcapsules.

Briefly, butyl methanesulfonate was synthesized by mixing butanol (1.0 mol) and triethylamine (1.0 mol) in dichloromethane (940 mL). Methanesulfonyl chloride (1.0 mol) was added, and the solution was kept at room temperature for two hours. The solution was washed with distilled water and dried with $MgSO_4$. The dichloromethane was evaporated, the produced ester was distilled, and a colorless liquid was achieved. Then, 1-*n*-butyl-3-methylimidazolium methanesulfonate was produced using butyl methanesulfonate (0.91 mol) and 1-methylimidazole (0.91 mol). After repeated recrystallization processes in acetone using previously prepared crystals of 1-*n*-butyl-3-methylimidazolium methanesulfonate as seeds, colorless crystals of 1-*n*-butyl-3-methylimidazolium methanesulfonate were synthesized. The final step to synthesize BMI.$NTf_2$ consisted of anion exchange by formulating two solutions: (1) lithium bis(trifluoromethanesulfonyl)imide (174 mmol) in distilled water (25 mL) and (2) 1-*n*-butyl-3-methylimidazolium methanesulfonate (165 mmol) in distilled water (65 mL). The solutions were mixed, stirred, and after phase separation, dichloromethane (200 mL) was added to facilitate removing the IL from the aqueous phase. The product was also washed with distilled water and dried with $MgSO_4$. The solvent was evaporated to obtain the characteristic colorless ionic liquid BMI.$NTf_2$ (yield of 98%).

After the synthesis of the ionic liquid BMI.$NTf_2$, microcapsules loaded with BMI.$NTf_2$ were synthesized (Fig. 2). First, 0.9 g of hydroxypropyl methylcellulose (METHOCEL - HPMC - F4M, Dow Pharma & Food Solutions, Midland, MI, USA) was mixed with 100 mL of ultrapure water. The solution was kept in the refrigerator at 4 °C for 24 h. Then, an organic phase was prepared with Eudragit S100 (Evonik Industries AG Pharma Polymers & Services, Kirschenallee, Darmstadt, Germany), poly (MMA-co-MAA) (0.50 g), ionic liquid BMI.$NTf_2$ (0.0160 g), and sorbitan monostearate (Span 60, Sigma-Aldrich Chemical, Inc., St. Louis, MO, USA) (0.19 g) dissolved in 125 mL of acetone (Nuclear, São Paulo, SP, Brazil) under magnetic stirring for 30 min at 37 °C. It was added in an aqueous phase composed of polysorbate 80 (Tween 80, Henrifarma, Sao Paulo, SP, Brazil) (0.385 g) and 200 mL of ultrapure water during constant stirring.

The HPMC dispersion was stirred at 37 °C, and the solution composed of the aqueous and organic phases were injected with a funnel into the HPMC dispersion while stirring. The final solution was dried using a Mini-Spray Dryer B-290 (BÜCHI Labortechnik AG, Flawi, Switzerland) with a dehumidifier (B-292, Buchi, Flawi, Switzerland). The feed pump rate of 5.0 mL $min^{-1}$ was used with 100% aspiration, 0.7 mm nozzle, atomization air at 819 L $h^{-1}$, and inlet temperature of 120 °C with a final outlet temperature of 70 °C. These temperatures are appropriate to remove the solvents, extracting residual liquids from the mixtures. The final product was characterized as a white powder (yield of approximately 42%).

### 2.2. Determination of particle size

The MC-IL powder was analyzed by laser diffraction (LD, Mastersizer 2000, Malvern Instruments, Worcestershire, UK) to obtain the average particle diameter (weighted average D4,3) and the polydispersity index (SPAN value) [28]. The powder formulation was analyzed directly using

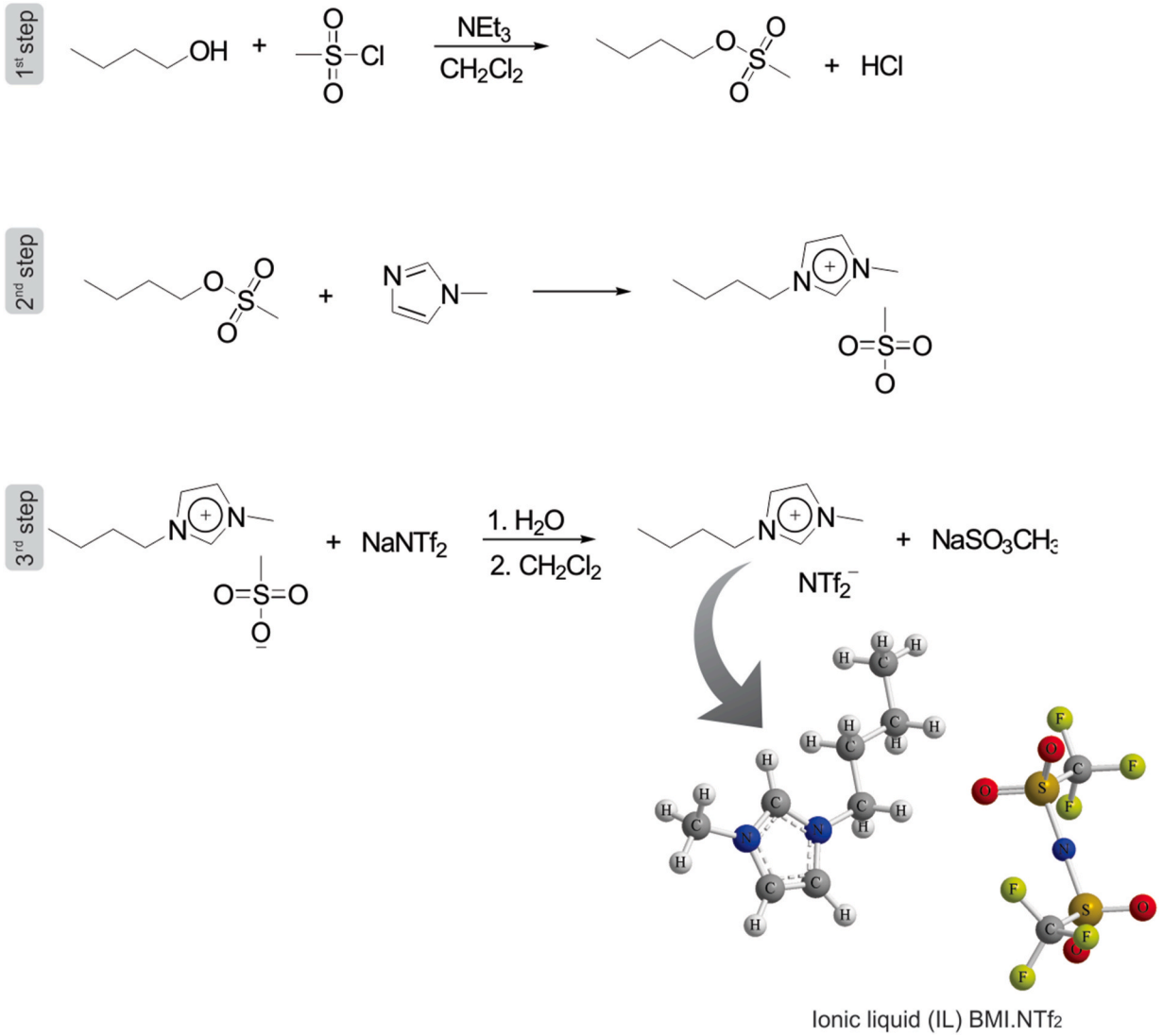


**Fig. 1.** Synthesis of the ionic liquid. The scheme displays the three steps for the ionic liquid (IL) BMI.$NTf_2$ synthesis and evidences the IL molecular structure.

a dry dispersion unit (Scirocco dry disperser, Malvern Instruments, Worcestershire, UK), with a stream of air being the dispersing medium (dry way). The refractive index used was 1.336, referred to as HPMC F4M. The laser obscuration was 2%. The results are expressed as a weighted average ($D_{(4.3)}$).

### 2.3. De-agglomeration analysis of particles

The powder's de-agglomeration profile was analyzed wet, using water as a dispersing medium and a rotation of 2000 rpm. Enough powder was added to the dispenser to obtain the laser's minimum obscuration, and particle size analyses were performed automatically for 30 min, at 5 min intervals. The refractive index used was 1.336, referred to HPMC F4M. The laser obscuration was 2%.

### 2.4. Morphological analysis

The MC-IL materials were analyzed by scanning electron microscopy (SEM). The synthesized powder of MC-IL was placed onto a metallic stub and gold-sputtered (15 - 25 nm of coat, SDC 050, Baltec, Vaduz, Liechtenstein). The SEM analysis (SEM, JSM 6060, Jeol, Tokyo, Japan) was performed at an accelerating voltage of 10 kV and 5,500x, 8,500x, and 13,000x magnification.

### 2.5. Formulation of resin infiltrants

The resin infiltrants were formulated by mixing 90 wt% of triethylene glycol dimethacrylates (TEGDMA) with 10 wt% of bisphenol A-glycidyl methacrylate (Bis-GMA) according to the previous study of resin infiltrant formulation [17]. A photoinitiator system composed of camphorquinone and ethyl 4-dimethylaminobenzoate were added at 1 mol%. The materials were purchased at Aldrich Chemical Co. (St. Louis, Missouri, USA). Four experimental resin infiltrants were prepared: base resin without MC-IL was used as a control group, and the other three groups were formulated with 2.5 wt%, 5 wt%, or 10 wt% by manually mixing the MC-IL with the base resin. The powder of MC-IL was kept in hermetically sealed flasks until use. The light-curing unit used was Radii Cal (SDI, Australia) with 1200 mW/cm$^2$, verified via the radiometer Ophir Optronics (Danvers, MA, USA).

### 2.6. Ultimate tensile strength (UTS)

The resin infiltrants were tested for ultimate tensile strength (UTS) using ten samples per group [29]. The samples were prepared in a metallic mold measuring 8.0 mm long, 2.0 mm wide, and 1.0 mm thickness. The mold presented an hourglass shape with 1 mm$^2$ of the constriction area. Uncured resin infiltrants were placed into the mold,

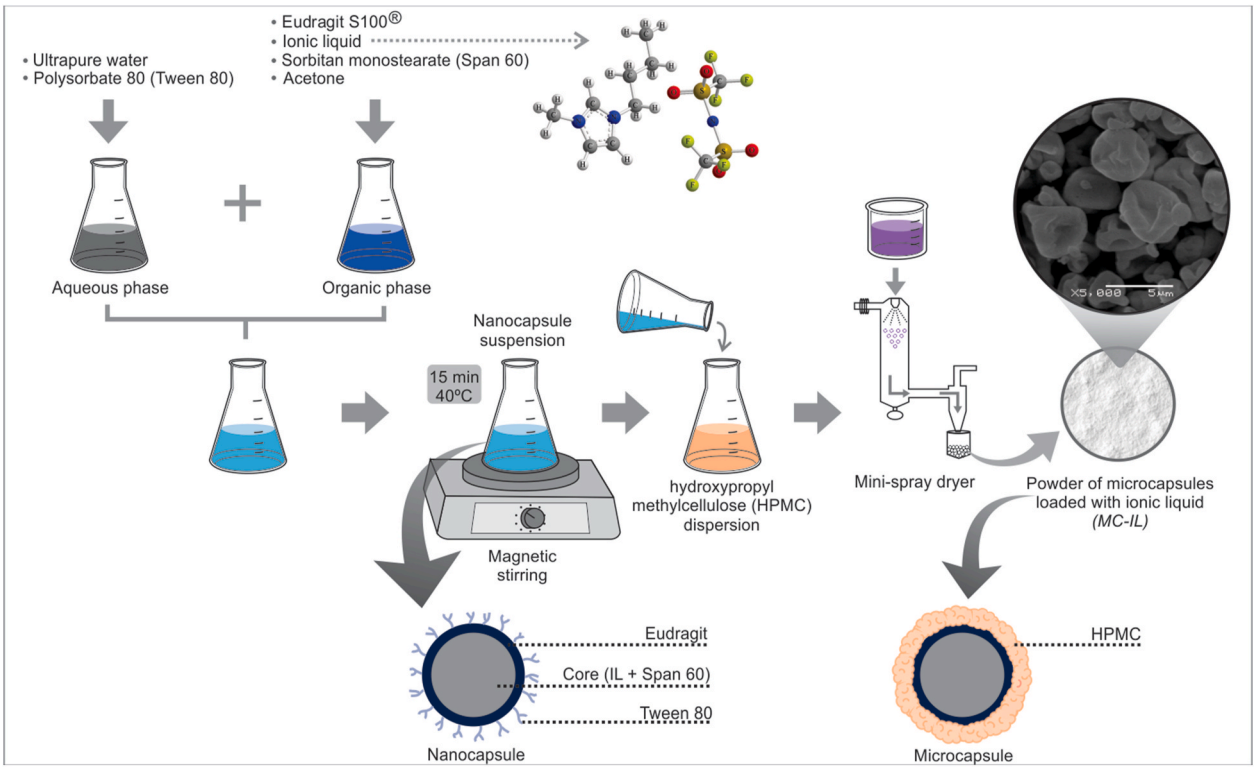


**Fig. 2.** Synthesis of the microcapsules loaded with ionic liquid (MC-IL). The scheme displays the steps to synthesize the MC-IL from the mixture of solutions up to drying. The colors of the solutions are illustrated in pink, grey, and red for better visual characterization. However, all solutions were colorless after the dissolution of the reagents. A white powder was obtained at the end of the process and then incorporated into the resin infiltrant at different concentrations. Part of the powder's scanning electron microscopy image was added in the figure to illustrate that microcapsules formed the powder generated with the indicated morphology. The scheme also describes the formation of the microcapsules and their composition at the bottom of the figure.

and a polyester strip (K-Dent, Biodental Produtos Dentários LTDA, Criciuma, SC, Brazil was used to cover the bottom and the top of each sample. The samples were photoactivated for 40 s on the bottom and 40 s on the top. During the photoactivation process, the beam of the light-curing unit was directly in contact with the sample surface, separated only by the thin and transparent polyester strip. The samples were carefully removed from the mold and immersed in 1.5 mL of distilled water at 37 °C for 24 h. The constriction area of each sample was measured with a digital caliper, and the samples were bonded into a metallic jig with cyanoacrylate adhesive. The samples were tested for tensile strength universal testing machine (EZ-SX Series, Shimadzu, Kyoto, Japan) with a crosshead speed of 1 mm/min until the fracture occurs in the constriction area. The results were expressed in megapascals (MPa) after dividing the force (Newtons) necessary to break each sample and its constriction area ($mm^2$).

### 2.7. Contact angle and surface free energy evaluation

Five samples per group [30] were prepared to measure 1.0 mm thickness and 6.0 mm in diameter to analyze the polymerized resin infiltrants' contact angle and surface free energy. Each uncured material was placed in circular molds and photoactivated for 40 s on the bottom and 40 s on the top. The light-curing unit's beam was directly in contact with the sample surface, separated only by the polyester strip. The samples were immersed in 1.5 mL of distilled water and kept at 37 °C in an incubator 24 h. The samples were embedded in self-curing acrylic resin and analyzed with an optical tensiometer Theta (Biolin Scientific, Stockholm, Sweden). Two results of the contact angle were acquired: with distilled water (polar liquid) or α-bromonaphtalene (non-polar liquid), by dropping these liquids on the polymerized infiltrant surface. Each drop of liquid tested had 3.0 μL, the drop rate used was 2.0 μL/s, with a displacement rate of 20.00 μL/s, and speed dispersion of 50 mm/min. The equipment monitored the contact angle from the moment of contact between the drop and the sample surface up to 20 s. The contact angle acquired at 10 s of contact between the drop and the surface was used as a result for contact angle with water or α-bromonaphtalene. With the contact angle values with water and contact angle with α-bromonaphtalene, the surface free energy (SFE) was calculated. For this purpose, the values recorded at 10 s after the contact of the drops with the sample's surface were used. The method applied to generate the SFE values was the Owens-Wendt-Rabel-Kaelble (OWRK) method [31] by OneAttension software (Biolin Scientific, Stockholm, Sweden).

### 2.8. Cytotoxicity evaluation

The viability of human keratinocytes (HaCaT, CLS Cell Lines Service GmbH, Eppelheim, Germany) was estimated by Sulforhodamine B (SRB) colorimetric assay. Five samples per group [21] (1.0 mm thickness x 4.0 mm diameter) were prepared after 40 s of photoactivation on the top and 40 s on the bottom. The light-curing unit's beam was directly in contact with the sample surface, separated only by the polyester strip. The samples were immersed in 1 mL of Dulbecco's Modified Eagle Medium (DMEM) for 24 h to prepare eluates. HaCaT cells were seeded at $5 \times 10^3$/well in 96-well plates, treated with 100 μL of eluates from each sample, and kept for 72 h at 37 °C in an incubator. Then, trichloroacetic acid (Sigma-Aldrich Chemical Co, St. Louis, Missouri, USA) at 10 vol.% was added to each well to fix the cells on the plates' bottom. After washing with water and dried at room temperature, the dye SRB (Sigma-Aldrich Chemical Co, St. Louis, Missouri, USA) at 0.4 vol.% was added into each well, and the plates were incubated at room temperature for 30 min. Acetic acid at 1 vol.% was used to wash the plates, which were dried at room temperature again. After the plates' complete dry, Trizma solution was added in the wells to resuspend the fixed cells.

After one hour at room temperature, each well's absorbance was analyzed at 560 nm via UV–Vis spectroscopy. The results were expressed as a percentage of viability in relation to the negative control (cells that were cultured in the absence of eluates).

### 2.9. Statistical analysis

The data were analyzed with the software SigmaPlot, version 12.0 (Systat Software, Inc., San Jose, CA, USA). MC-IL characterization via the laser-diffraction method and SEM were descriptively analyzed. The data distribution of resin infiltrant's analyses was evaluated with the Shapiro-Wilk test. The results of UTS, contact angle with water, the contact angle with α-bromonaphtalene, and surface free energy were analyzed via one-way ANOVA. Tukey's post hoc test was applied when a statistical difference was observed. Cytotoxicity was analyzed via Kruskal-Wallis. A significant level of 5% was used for all tests.

## 3. Results

The MC-IL synthesized from the interfacial deposition of preformed polymers showed a mean particle size of 1.64 (±0.08) μm and a SPAN value of 1.02 (±0.03). Fig. 3 represents the granulometric dispersion profile of the MC-IL powder, using air or water as a dispersing medium. The dry analysis (Fig. 3 - solid grey line) shows that the synthesized MC-IL is uniform, monomodal, with a narrow particle size range, constituted mainly by microparticles (10% of the particles <1 μm). The wet analysis provides an estimate of how the material tends to behave when it comes in contact with a liquid medium (Fig. 3 - T1 and T7). The graph shows the particles' shift towards the nanometric range, with two populations of particles over time: micro and nanoparticles. Table 1 shows the 10th percentile, 50th percentile, and 90th percentile of the MC-IL in the dry and wet analyses.

The SEM analysis confirmed the micrometer scale size of the particles showed by laser diffraction analysis (Fig. 4). Besides, the particles presented a biconcave disc shape with invaginations and shriveled aspect.

**Table 1**
Percentiles of the size distribution (diameter) of the synthesized MC-IL in the dry dispersion and after the contact with water for 15 min (T1) and 30 min (T1). The analyses were performed using the laser diffraction method, and the results are expressed in micrometers (μm).

| Sample | 10th | 50th | 90th |
|---|---|---|---|
| MC-IL (dry dispersion) | 0.935 | 1.545 | 2.522 |
| MC-IL (T1) | 0.077 | 0.158 | 0.600 |
| MC-IL (T7) | 0.071 | 0.147 | 0.343 |

Table 2 displays UTS results, the contact angle with water, the contact angle with α-bromonaphtalene, and surface free energy. UTS results ranged from 62.13 (±6.80) for the group containing 2.5 wt% of MC-IL to 69.88 (±9.08) for the group containing 10 wt% of MC-IL. There was no statistically significant difference among the groups for the UTS test ($p > 0.05$).

The contact angle with water ranged from 62.16 (±2.11) for the control group to 77.87 (±4.73) for 10 wt% addition of MC-IL. The group with 10 wt% showed a higher contact angle in comparison to all other groups ($p < 0.05$), and there was no difference from control to 5 wt% ($p > 0.05$). The contact angle results with α-bromonaphtalene showed no statistically significant differences among groups from control to 5 wt% of MC-IL ($p > 0.05$). The incorporation of 10 wt% of MC-IL increased the contact angle from 11.07 (±2.66) for the control group to 35.04 (±4.49), with a statistically significant difference for 10 wt% of MC-IL in comparison to all other groups ($p < 0.05$).

From 5 wt% of MC-IL addition, there was a statistically significant difference for SFE compared to the control group ($p < 0.05$). With 5 wt %, the SFE decreased from 55.85 (±5.37) for the control group to 49.70 (±1.57) ($p < 0.05$). When 10 wt% of MC-IL was added, the SFE decreased to 41.66 (±2.46) ($p < 0.05$).

The cytotoxicity results are displayed in Fig. 5. All mean values were

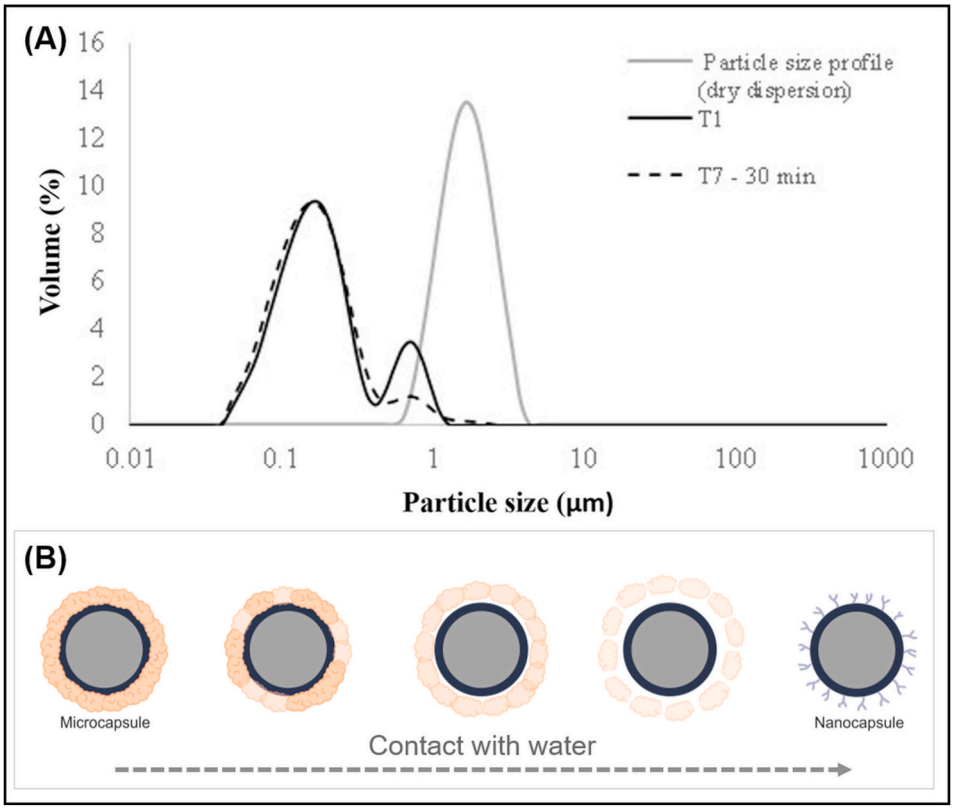


**Fig. 3.** Particle size analysis by laser diffraction. In the image A, the solid grey line represents the particle size profile in a dry dispersion. The solid black line represents the particle size profile in the de-agglomeration analysis, using water as a dispersion medium after 15 min (T1) and 30 min (T7) of contact between powder of MC-IL and water. The black dashed line represents the particle size profile in the de-agglomeration analysis, using water as a dispersion medium, after 30 min of contact between powder and water. In the image B, a illustration shows how the plasticizing effect of the polymeric chains of HPMC probably occurs up to the loss of HPMC and release of the nanocapsules from the microcapsules.

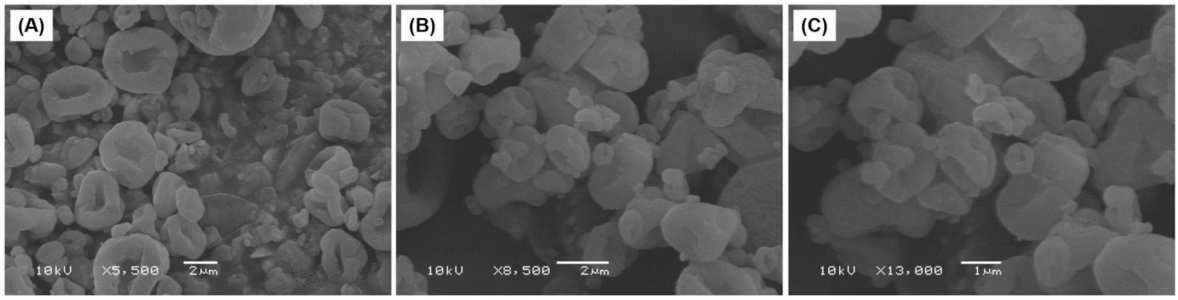


**Fig. 4.** SEM images of synthesized MC-IL. Image (A) shows the MC-IL with 5,000x magnification, image B shows with 8,500x magnification, and image C with 13,000x magnification.

**Table 2**
Mean and standard deviation values of ultimate tensile strength (UTS), contact angle with water or α-bromonaphtalene, and surface free energy (SFE).

| Groups | UTS (MPa) | Contact Angle | | SFE (mN/M) |
|---|---|---|---|---|
| | | Water | α-bromonaphtalene | |
| Control | 65.67 (±4.97) $^{A}$ | 62.16 (±2.11) $^{B}$ | 11.07 (±2.66) $^{B}$ | 53.50 (±1.21) $^{A}$ |
| 2.5% MC-IL | 62.13 (±6.80) $^{A}$ | 65.74 (±3.81) $^{B}$ | 18.31 (±8.26) $^{B}$ | 50.71 (±1.91) $^{AB}$ |
| 5% MC-IL | 63.40 (±7.12) $^{A}$ | 68.66 (±3.23) $^{B}$ | 17.08 (±2.95) $^{B}$ | 49.70 (±1.57) $^{B}$ |
| 10% MC-IL | 69.88 (±9.08) $^{A}$ | 77.87 (±4.73) $^{A}$ | 35.04 (±4.49) $^{A}$ | 41.66 (±2.46) $^{C}$ |

Different capital letters indicate a statistically significant difference in the same column ($p < 0.05$).

higher than 90% of cell viability. The values ranged from 109.68 (±0.52) % for 2.5 wt% of MC-IL to 91.23 (±1.72) % for 10 wt% of MC-IL.

## 4. Discussion

Microinvasive technique with resin infiltrants is effective in managing non-cavitated carious lesions in proximal surfaces [32]. Along with oral hygiene instructions, the use of resin infiltrants has been recommended to hamper carious progression in areas up to the outer third of dentin [32]. In this study, a resin infiltrant with promising therapeutic effects was formulated with microcapsules loaded with a new antibacterial agent composed of IL. The developed material showed improved surface properties without impacts on mechanical and cytotoxicity properties.

The MC-IL were prepared via a self-assembly process [28,33] (Fig. 2). The microcapsules synthesized are methacrylate-derived materials, which assists in the compatibility with the methacrylate-based resin used to formulate the resin infiltrants. Two amphiphilic surfactants were used because polysorbate 80 is polar and sorbitan monostearate is non-polar. This change in the hydrophilic/hydrophobic property assists in conferring the shape and stability of the particles. An interesting difference between the synthesis used here compared to others previously reported [34,35] is that due to IL's high hydrophobicity, it was possible to synthesize the particles without additional oils as capric and caprylic triglycerides. These oils usually are necessary as adjuvants in the formation of the microcapsules' core.

The MC-IL here reported were formed by a core of IL surrounded by a polymeric wall of methacrylate and methacrylic acid (Eudragit S100). The surface of the MC-IL was shriveled, as previously shown [33]. It was attributed to hydroxypropyl methylcellulose (HPMC), which was used as a drying aid [33]. During the drying process, the suspension of synthesized particles incorporated into the HPMC dispersion is conducted to the spray drying. The mini spray dryer's equipment atomizer produces a fine mist of sprayed droplets, and the droplets are dried by hot air. Each droplet generated is composed of MC-IL, HPMC, acetone, and water. The HPMC increases the formulation's viscosity, and in contact with the high temperature, it quickly dries, forming a thin dry film around the droplets (Fig. 6). The residual liquid inside the partially dried droplet is extracted by capillarity due to the high external temperature and high internal pressure. At the end of this process, the collected powder consists of microcapsules with irregularities on its surface due to the wilting process, leading to a shriveled aspect observed in SEM (Fig. 4). The MC-IL synthesis route was reproducible and resulted in particles of micrometric size with a mean size of 1.64 (±0.08) μm. The laser diffraction analysis also showed a monomodal behavior and a narrow range of particle size distribution, as observed by the low polydispersion index (SPAN = 1.02 ± 0.03), suggesting uniformity particles in a dry powder.

The particle size profile in the dry environment shows one single peak on the micrometer scale. However, when dispersed in water, the profile is different, with the formation of two peaks (Fig. 3). The study of the particles in an aqueous medium (de-agglomeration analysis) better reveals the particles' size profile, showing that the powder is composed of nanoparticles with different sizes instead of only micrometric particles. The pattern observed in Fig. 1 is mostly related to HPMC behavior. Probably the release of the agents occur in the following order: immediately after HPMC-aqueous medium contact, there is partial solubilization of the HPMC film that surrounds the MC-IL, releasing some of the nanoparticles and leading to the formation of two peaks in the graph related to free nanoparticles with different sizes (T1); then, HPMC swells and acts as a barrier that delays the nanoparticles release, leading to the decrease of peak heigh related to free larger nanoparticles (T7). After a more extended period of contact with water, higher plasticization and degradation occur for HPMC chains, causing erosion process and release of more nanoparticles. The coating of methacrylate and methacrylic acid (Euragit) needs to be further eroded for IL release. In this way, the polymeric barriers provide the slow release property of the encapsulated agent. After 30 min in the same medium (T7), the particle size profile maintenance confirms the prone of the additional barrier be maintained and probably delay the release of the encapsulated drug [33].

In this study, we analyzed the UTS of the formulated resin infiltrants because this property could impact white-spot lesions' stability or even act to reinforce the demineralized area. The incorporation of particles in the resin matrix may change the mechanical behavior of the polymer. In resin materials with low viscosity, fillers' concentration is usually up to 15 wt% to attain excellent viscosity and penetrability in demineralized enamel sites [36,37]. MC-IL were added from 2.5 to 10 wt% in the organic matrix following a pilot study. The authors observed that the infiltrants remained with proper handling regardless of the particle concentration. The addition of MC-IL did not change the mechanical behavior of the infiltrants. The maintenance of the tensile strength values is probably attributed to similar polymeric network formation. The polymeric microcapsules have no reactivity within the organic matrix since it is covered by a copolymer and HPMC, which may not confer energy to modify polymerization kinetics. Moreover, the stabilizing agent HPMC adsorbed on MC-IL may help grant the MC-IL and

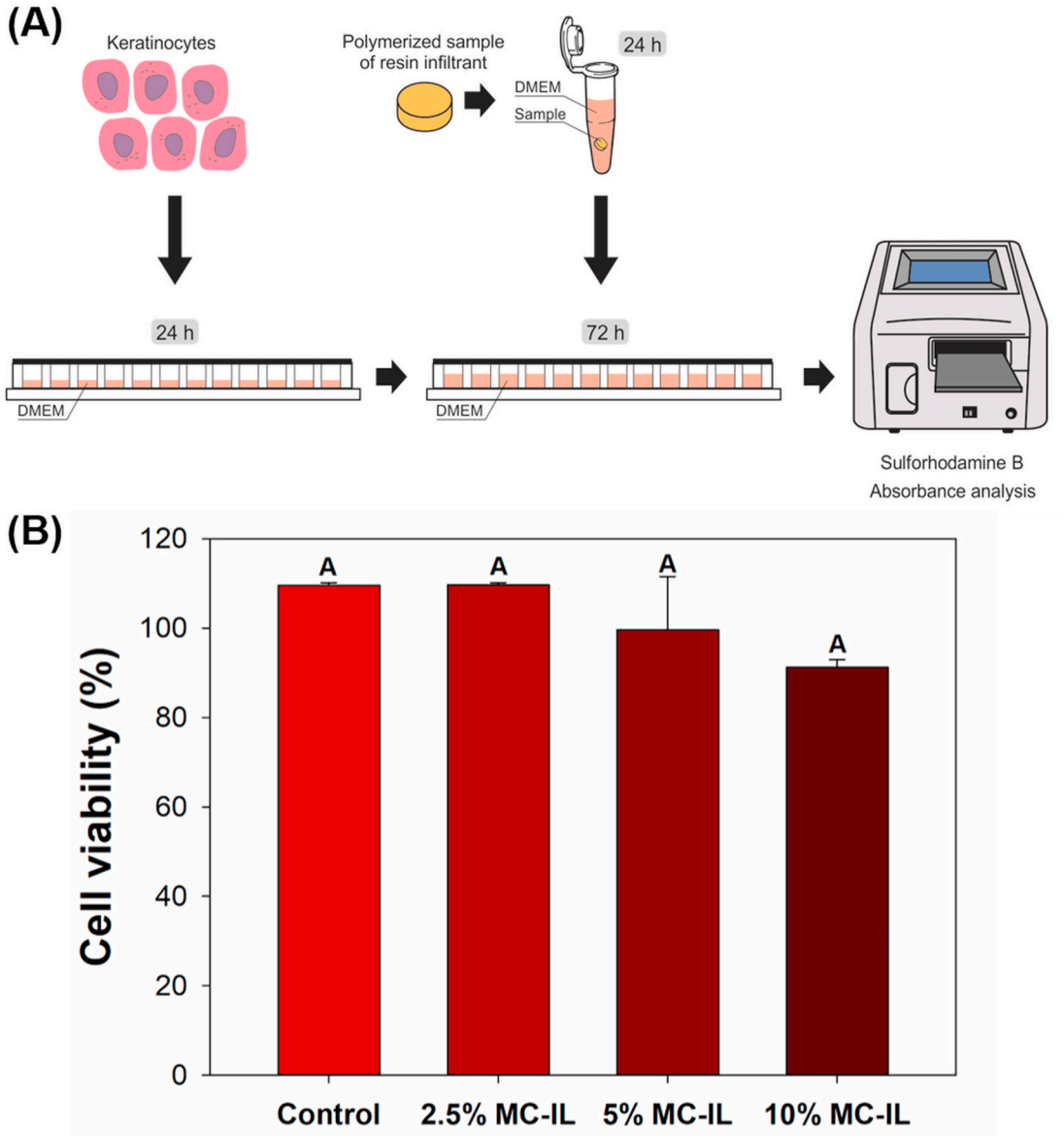


**Fig. 5.** Image (A) illustrates the cytotoxicity methodology. Image (B) shows the mean and standard deviation values of cell viability for each resin infiltrants group after the cytotoxicity test. The same letters indicate no statistical difference among groups ($p > 0.05$).

organic matrix's chemical affinity, favoring tensile transfer processes.

In addition to mechanical behavior, the experimental dental resins were tested for surface properties. The modification of organic resin may modify the contact angle and the SFE of the developed polymer. The test performed in the present study is based on the contact angle formed among the complex solid-liquid-air, where the solid surface consists of the polymerized resin infiltrant, and the liquid was distilled water or α-bromonaphtalene. The addition of 10 wt% of MC-IL increased the contact angle and decreased the SFE of the resin infiltrant in comparison to the control group. The contact angle and the SFE are related to the materials' hydrophilicity and may help predict behaviors related to water sorption [38]. Therefore, the interaction of materials surface and the medium around them can be investigated using this test. A higher contact angle and decreased SFE makes the material less prone to be wet. This feature is interesting since the higher hydrophobicity and lower wettability of polymers may favor hydrolytic stability in the oral environment.

The effect of the contact angles and SFE on bacterial colonization has been investigated. Some studies report that the increased contact angle and decreased SFE may lead to an antibiofilm effect. These changes make the material alter from hydrophilic to hydrophobic, reducing the bacterial attachment [39–41]. However, the results of this theme are controversial. Almaroof et al. [38] discussed this issue, stating that the non-clear consensus remains that bacterial adherence is complex. It is not related only to the physical property of the surface but also to its chemical composition. Besides the solid's physical and chemical properties, the liquid surrounding and growing broth and the type of bacteria probably influence the outcomes [38]. However, it is interesting to observe that at least 5 wt% of MC-IL changed the SFE. In addition to the antibacterial activity of the IL BMI.$NTf_2$, bacterial adherence could be diminished because of the change in these properties. It is a limitation of this study not to have tested the antimicrobial activity of the formulated materials.

ILs were already used to create antibacterial coatings in polymers [42] and nanoparticles [19,20,43]. Moreover, dicationic imidazolium-based ILs with $NTf_2$ were used to provide antibacterial property, anti-corrosion characteristics, and lubrication to implants surfaces [44,45]. BMI.$NTf_2$ used as a core of the present study's microcapsules already showed antibacterial activity against biofilm formation of *S. mutans* and planktonic *S. mutans* [21]. In these previous

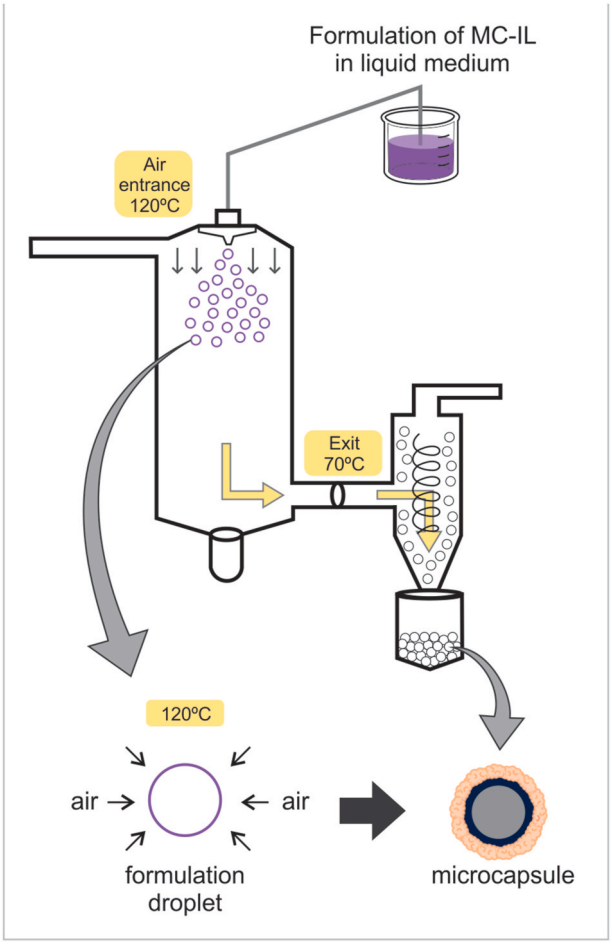


**Fig. 6.** Schematic illustration of the dry process of the MC-IL.

analyses, a dental adhesive was placed in contact with this bacterium, and it was demonstrated that probably the IL had leached from the polymer matrix, decreasing the viability of *S. mutans* in these two stages (biofilm and planktonic) [21]. Another interesting question to be addressed is if there is any difference between dental resins with free IL and dental resins with MC-IL. Usually, the use of encapsulated drugs reduces the quantity of antibacterial agents necessary for the activity [46]. The present study is the first attempt to encapsulate an IL and apply this platform in a dental material. It is beyond the scope of this study to analyze all the issues mentioned above. Future studies are encouraged to investigate the antibacterial activity of dental materials with MC-IL and analyze if the SFE and contact angle differences could interfere with the antibacterial property. Furthermore, *in situ* studies [47] applying the infiltrants in enamel is an exciting future study to translate the knowledge from the bench to the clinical setting.

Finally, the infiltrants were tested against human keratinocytes. The cytotoxicity assay was performed via the staining method using SRB dye [48]. Previous studies have already tested the potential cytotoxic effect of nanocapsules and microspheres, synthesized via similar routes, in adhesives [49,50], sealers [51], and endodontic paste [28]. When tested *in vitro*, the assays were performed with pulp cells due to the clinical indication that those materials had. In the present investigation, the infiltrants were tested against keratinocytes due to this material's possible contact in teeth' proximal surfaces with keratinocytes. ISO preconizes that at least 70% of cell viability is expected for non-cytotoxic materials [52]. Average and median values were above 90% for all groups, suggesting no cytotoxic effect against the human cells. HPMC, the more external layer around the microcapsules, forms a diffusion barrier for the components loaded, extending the drug release profile [33]. It probably assists in overcoming the cytotoxic effects of drugs loaded. Moreover, HPMC is biocompatible, which is an essential feature in drug release systems [33].

Overall, MC-IL incorporation changed the resin infiltrants' surface properties without affecting the polymer's tensile strength and cytotoxicity. Initial results on the feasibility of formulating new resin infiltrants were reported to improve micro-invasive treatments further.

## 5. Conclusion

In this study, microcapsules loaded with ionic liquid were successfully synthesized and incorporated into an experimental resin infiltrant. The incorporation of at least 5 wt% of MC-IL decreased the polymer's SFE without changing its tensile strength and cytotoxic effect. MC-IL may be a promising strategy to improve materials for restorative and micro-invasive dental treatments.

## Funding

This research did not receive any specific grant from funding agencies in the public, commercial, or not-for-profit sectors.

## CRediT authorship contribution statement

**Marla Cuppini:** Conceptualization, Formal analysis, Investigation. **Isadora Martini Garcia:** Conceptualization, Formal analysis, Investigation, Writing - original draft. **Virgínia Serra de Souza:** Investigation, Visualization, Writing - review & editing. **Kelly Cristine Zatta:** Formal analysis, Investigation, Writing - review & editing. **Fernanda Visioli:** Investigation, Supervision. **Vicente Castelo Branco Leitune:** Supervision. **Sílvia Stanisçuazki Guterres:** Supervision. **Jackson Damiani Scholten:** Supervision, Visualization, Writing - review & editing. **Fabrício Mezzomo Collares:** Conceptualization, Supervision, Writing - review & editing.

## Declaration of competing interest

None.

## Acknowledgments

The authors gratefully acknowledge Microscopy and Microanalysis Center (Federal University of Rio Grande do SulFederal University of Rio Grande do Sul) for the scanning electron microscopy images. This study was financed in part by the Coordenação de Aperfeiçoamento de Pessoal de Nível Superior - Brasil (CAPES) - Finance Code 001, and Conselho Nacional de Desenvolvimento Científico e Tecnológico – Brasil (CNPq) – n° 307095/2016-9.

## References

[1] G.O.D. Collaborators, Global, Regional, and National Levels and Trends in Burden of Oral Conditions from 1990 to 2017: A Systematic Analysis for the Global Burden of Disease 2017 Study, vol. 99, 2020, pp. 362–373.
[2] S.O. Griffin, J.A. Jones, D. Brunson, P.M. Griffin, W.D. Bailey, Burden of oral disease among older adults and implications for public health priorities, Am. J. Publ. Health 102 (2012) 411–418.
[3] M. Anderson, C. Stecksén-Blicks, H. Stenlund, L. Ranggård, G. Tsilingaridis, I. Mejàre, Detection of approximal caries in 5-year-old Swedish children, Caries Res. 39 (2005) 92–99.
[4] J.A. Cury, L.M. Tenuta, Enamel remineralization: controlling the caries disease or treating early caries lesions? Braz. Oral Res. 23 (Suppl 1) (2009) 23–30.
[5] C. Cumerlato, F.F. Demarco, A.J.D. Barros, M.A. Peres, K.G. Peres, A. Morales Cascaes, et al., Reasons for direct restoration failure from childhood to adolescence: a birth cohort study, J. Dent. 89 (2019) 103183.
[6] A.M. Kielbassa, I. Ulrich, R. Schmidl, C. Schüller, W. Frank, V.D. Werth, Resin infiltration of deproteinised natural occlusal subsurface lesions improves initial quality of fissure sealing, Int. J. Oral Sci. 9 (2017) 117–124.
[7] H. Meyer-Lueckel, S. Paris, Progression of artificial enamel caries lesions after infiltration with experimental light curing resins, Caries Res. 42 (2008) 117–124.

[8] S. Paris, K. Bitter, J. Krois, H. Meyer-Lueckel, Seven-year-efficacy of proximal caries infiltration - randomized clinical trial, J. Dent. 93 (2020) 103277.
[9] S. Paris, V.M. Soviero, A.J. Chatzidakis, H. Meyer-Lueckel, Penetration of experimental infiltrants with different penetration coefficients and ethanol addition into natural caries lesions in primary molars, Caries Res. 46 (2012) 113–117.
[10] K.R. Ekstrand, A. Bakhshandeh, S. Martignon, Treatment of proximal superficial caries lesions on primary molar teeth with resin infiltration and fluoride varnish versus fluoride varnish only: efficacy after 1 year, Caries Res. 44 (2010) 41–46.
[11] H. Meyer-Lueckel, A. Balbach, C. Schikowsky, K. Bitter, S. Paris, Pragmatic RCT on the efficacy of proximal caries infiltration, J. Dent. Res. 95 (2016) 531–536.
[12] S. Imazato, Antibacterial properties of resin composites and dentin bonding systems, Dent. Mater. 19 (2003) 449–457.
[13] M.S. Ibrahim, A.A. Balhaddad, I.M. Garcia, E. Hefni, F.M. Collares, F.C. Martinho, et al., Tooth sealing formulation with bacteria-killing surface and on-demand ion release/recharge inhibits early childhood caries key pathogens, J. Biomed. Mater. Res. B Appl. Biomater. (2020).
[14] M.S. Ibrahim, I.M. Garcia, T. Vila, A.A. Balhaddad, F.M. Collares, M.D. Weir, et al., Multifunctional antibacterial dental sealants suppress biofilms derived from children at high risk of caries, Biomater. Sci. 8 (2020) 3472–3484.
[15] A.M. Kielbassa, M.R. Leimer, J. Hartmann, S. Harm, M. Pasztorek, I.B. Ulrich, Ex vivo investigation on internal tunnel approach/internal resin infiltration and external nanosilver-modified resin infiltration of proximal caries exceeding into dentin, PloS One 15 (2020), e0228249.
[16] J. Yu, X. Huang, X. Zhou, Q. Han, W. Zhou, J. Liang, et al., Anti-caries effect of resin infiltrant modified by quaternary ammonium monomers, J. Dent. 97 (2020) 103355.
[17] F.M. Collares, I.M. Garcia, F.R. Bohns, A. Motta, M.A. Melo, V.C.B. Leitune, Guanidine hydrochloride polymer additive to undertake ultraconservative resin infiltrant against Streptococcus mutans, Eur. Polym. J. 133 (2020) 109746.
[18] L.T. Inagaki, R.C. Alonso, G.A. Araujo, E.J. de Souza-Junior, P.C. Anibal, J. F. Hofling, et al., Effect of monomer blend and chlorhexidine-adding on physical, mechanical and biological properties of experimental infiltrants, Dent. Mater. 32 (2016) e307–e313.
[19] I.M. Garcia, V.S. Souza, C. Hellriegel, J.D. Scholten, F.M. Collares, Ionic liquid-stabilized titania quantum dots applied in adhesive resin, J. Dent. Res. 98 (2019) 682–688.
[20] I.M. Garcia, V.S. Souza, J.D. Scholten, F.M. Collares, Quantum dots of tantalum oxide with an imidazolium ionic liquid as antibacterial agent for adhesive resin, J. Adhesive Dent. 22 (2020) 207–214.
[21] I. Martini Garcia, Ferreira C. Jung, V.S. de Souza, V. Castelo Branco Leitune, S.M. W. Samuel, G. de Souza Balbinot, et al., Ionic liquid as antibacterial agent for an experimental orthodontic adhesive, Dent. Mater. 35 (2019) 1155–1165.
[22] J.N. P, B.F. G, The antimicrobial potential of ionic liquids: a source of chemical diversity for infection andbiofilm control, Int. J. Antimicrob. Agents 46 (2015) 131–139.
[23] J. Dupont, R.F.d. Souza, P.A.Z. Suarez, Ionic liquid (molten salt) phase organometallic catalysis, Chem. Rev. 102 (2003) 3667–3692.
[24] R. Ferraz, L.C. Branco], C. Prudêncio, J.P. Noronha, Z. Petrovski, Ionic liquids as active pharmaceutical ingredients, ChemMedChem 6 (2011) 975–985.
[25] B. Genari, V.C.B. Leitune, D.S. Jornada, M. Camassola, R.A. Arthur, A.R. Pohlmann, et al., Antimicrobial effect and physicochemical properties of an adhesive system containing nanocapsules, Dent. Mater. 33 (2017) 735–742.
[26] B. Genari, V.C.B. Leitune, D.S. Jornada, B.R. Aldrigui, A.R. Pohlmann, S. S. Guterres, et al., Effect on adhesion of a nanocapsules-loaded adhesive system, Braz. Oral Res. 32 (2018) e008.
[27] C. Cc, E. G, F. B, J. D, A simple and practical method for the preparation and purity determination of halide-free imidazolium ionic liquids, Adv. Synth. Catal. 348 (2006) 243–248.
[28] M. Cuppini, K.C. Zatta, L.B. Mestieri, F.S. Grecca, V.C.B. Leitune, S.S. Guterres, et al., Antimicrobial and anti-inflammatory drug-delivery systems at endodontic reparative material: synthesis and characterization, Dent. Mater. 35 (2019) 457–467.
[29] P.A. Mena Silva, I.M. Garcia, J. Nunes, F. Visioli, V. Castelo Branco Leitune, M. A. Melo, et al., Myristyltrimethylammonium bromide (MYTAB) as a cationic surface agent to inhibit Streptococcus mutans grown over dental resins: an in vitro study, J. Funct. Biomater. 11 (2020).
[30] J.C. Monteiro, M. Stürmer, I.M. Garcia, M.A. Melo, S. Sauro, V.C.B. Leitune, et al., Dental sealant empowered by 1,3,5-tri acryloyl hexahydro-1,3,5-triazine and α-tricalcium phosphate for anti-caries application, Polymers 12 (2020).
[31] O. Dk, W. Rc, Estimation of the surface free energy of polymers, J. Appl. Polym. Sci. 13 (1969) 1741–1747.
[32] S. Chatzimarkou, D. Koletsi, K. Kavvadia, The effect of resin infiltration on proximal caries lesions in primary and permanent teeth. A systematic review and meta-analysis of clinical trials, J. Dent. 77 (2018) 8–17.
[33] K.C. Zatta, L.A. Frank, L.A. Reolon, L. Amaral-Machado, E.S.T. Egito, M.P. D. Gremiao, et al., An inhalable powder formulation based on micro- and nanoparticles containing 5-fluorouracil for the treatment of metastatic melanoma, Nanomaterials 8 (2018).
[34] E.A. Bender, M.D. Adorne, L.M. Colomé, D.S.P. Abdalla, S.S. Guterres, A. R. Pohlmann, Hemocompatibility of poly(ε-caprolactone) lipid-core nanocapsules stabilized with polysorbate 80-lecithin and uncoated or coated with chitosan, Int. J. Pharm. 426 (2012) 271–279.
[35] E. Jäger, C.G. Venturini, F.S. Poletto, L.M. Colomé, J.P. Pohlmann, A. Bernardi, et al., Sustained release from lipid-core nanocapsules by varying the core viscosity and the particle surface area, J. Biomed. Nanotechnol. 5 (2009) 130–140.
[36] R.A. Sfalcin, A.B. Correr, L.R. Morbidelli, T.G.F. Araujo, V.P. Feitosa, L. Correr-Sobrinho, et al., Influence of bioactive particles on the chemical-mechanical properties of experimental enamel resin infiltrants, Clin. Oral Invest. 21 (2017) 2143–2151.
[37] K.L. Van Landuyt, J. Snauwaert, J. De Munck, M. Peumans, Y. Yoshida, A. Poitevin, et al., Systematic review of the chemical composition of contemporary dental adhesives, Biomaterials 28 (2007) 3757–3785.
[38] A. Almaroof, S.A. Niazi, L. Rojo, F. Mannocci, S. Deb, Influence of a polymerizable eugenol derivative on the antibacterial activity and wettability of a resin composite for intracanal post cementation and core build-up restoration, Dent. Mater. 32 (2016) 929–939.
[39] Zaltsman Nathan, Andrei C. Ionescu, Ervin I. Weiss, Eugenio Brambilla, Shaul Beyth, N. Beyth, Surface-modified nanoparticles as anti-biofilm filler for dental polymers, PloS One 12 (2016), e0189397.
[40] Y. Liu, Q. Zhao, Influence of surface energy of modified surfaces on bacterial adhesion, Biophys. Chem. 117 (2005) 39–45.
[41] R. Buergers, W. Schneider-Brachert, S. Hahnel, M. Rosentritt, G. Handel, Streptococcal adhesion to novel low-shrink silorane-based restorative, Dent. Mater. 25 (2009) 269–275.
[42] B. R, Z. Z, L. Y, T. H, Z. J, Q. W, et al., A facile antibacterial coating based on UV-curable acrylatedimidazoliums, J. Coating Technol. Res. 15 (2018) 345–349.
[43] A. Abbaszadegan, M. Nabavizadeh, A. Gholami, Z.S. Aleyasin, S. Dorostkar, M. Saliminasab, et al., Positively charged imidazolium-based ionic liquid-protected silver nanoparticles: a promising disinfectant in root canal treatment, Int. Endod. J. 48 (2015) 790–800.
[44] G. Im, S. Da, F. Cp, M. Map, D.C. Rodrigues, Improvement of tribological and anti-corrosive performance of titanium surfaces coated with dicationicimidazolium-based ionic liquids, RSC Adv. 6 (2016) 78795–78802.
[45] G. Im, P. Kl, S. Da, A. S, F. Cp, M. Map, et al., Evaluation of mammalian and bacterial cell activity on titanium surface coated with dicationicimidazolium-based ionic liquids, RSC Adv. 6 (2016) 36475–36483.
[46] S.R. Schaffazick, S.S. Guterres, L.d.L. Freitas, A.R. Pohlmann, Caracterização e estabilidade físico-química de sistemas poliméricos nanoparticulados para administração de fármacos, Quim. Nova 26 (2003) 726–737.
[47] F.W. Degrazia, A.S.P. Altmann, C.J. Ferreira, R.A. Arthur, V.C.B. Leitune, S.M. W. Samuel, et al., Evaluation of an antibacterial orthodontic adhesive incorporated with niobium-based bioglass: an in situ study, Braz. Oral Res. 33 (2019), e010.
[48] A. van Tonder, A.M. Joubert, A.D. Cromarty, Limitations of the 3-(4,5-dimethylthiazol-2-yl)-2,5-diphenyl-2H-tetrazolium bromide (MTT) assay when compared to three commonly used cell enumeration assays, BMC Res. Notes 8 (2015) 47.
[49] B. Genari, M.B.C. Ferreira, L.F. Medeiros, J.S. de Freitas, S.G. Cioato, I.L. da Silva Torres, et al., Anti-inflammatory effect of an adhesive resin containing indomethacin-loaded nanocapsules, Arch. Oral Biol. 84 (2017) 106–111.
[50] B. Genari, V.C. Leitune, D.S. Jornada, M. Camassola, A.R. Pohlmann, S.S. Guterres, et al., Effect of indomethacin-loaded nanocapsules incorporation in a dentin adhesive resin, Clin. Oral Invest. 21 (2017) 437–446.
[51] N.B.J. Dornelles, F.M. Collares, B. Genari, G. de Souza Balbinot, S.M.W. Samuel, R. A. Arthur, et al., Influence of the addition of microsphere load amoxicillin in the physical, chemical and biological properties of an experimental endodontic sealer, J. Dent. 68 (2018) 28–33.
[52] International Organization for Standardization, ISO 10993-5:2009. Biological Evaluation of Medical Devices – Part 5: Tests for in Vitro Cytotoxicity, 2009, pp. 1–34.